Peptide-mediated desmoglein 3 crosslinking prevents pemphigus vulgaris autoantibody-induced skin blistering

Volker Spindler,[1,2] Vera Rötzer,[1] Carina Dehner,[1] Bettina Kempf,[2] Martin Gliem,[2] Mariya Radeva,[1] Eva Hartlieb,[1] Gregory S. Harms,[3,4] Enno Schmidt,[5,6] and Jens Waschke[1,2]

[1]Institute of Anatomy and Cell Biology, Ludwig-Maximilians-Universität, Munich, Germany. [2]Institute of Anatomy and Cell Biology and [3]Bioimaging Center, Rudolf Virchow Center, Julius-Maximilians-Universität, Würzburg, Germany. [4]Department of Biology and Physics, Wilkes University, Wilkes-Barre, Pennsylvania, USA. [5]Department of Dermatology and [6]Comprehensive Center for Inflammation Medicine, University of Lübeck, Lübeck, Germany.

In pemphigus vulgaris, a life-threatening autoimmune skin disease, epidermal blisters are caused by autoantibodies primarily targeting desmosomal cadherins desmoglein 3 (DSG3) and DSG1, leading to loss of keratinocyte cohesion. Due to limited insights into disease pathogenesis, current therapy relies primarily on nonspecific long-term immunosuppression. Both direct inhibition of DSG transinteraction and altered intracellular signaling by p38 MAPK likely contribute to the loss of cell adhesion. Here, we applied a tandem peptide (TP) consisting of 2 connected peptide sequences targeting the DSG adhesive interface that was capable of blocking autoantibody-mediated direct interference of DSG3 transinteraction, as revealed by atomic force microscopy and optical trapping. Importantly, TP abrogated autoantibody-mediated skin blistering in mice and was effective when applied topically. Mechanistically, TP inhibited both autoantibody-induced p38 MAPK activation and its association with DSG3, abrogated p38 MAPK-induced keratin filament retraction, and promoted desmosomal DSG3 oligomerization. These data indicate that p38 MAPK links autoantibody-mediated inhibition of DSG3 binding to skin blistering. By limiting loss of DSG3 transinteraction, p38 MAPK activation, and keratin filament retraction, which are hallmarks of pemphigus pathogenesis, TP may serve as a promising treatment option.

Introduction

Pemphigus vulgaris (PV) is a life-threatening blistering disease histopathologically characterized by acantholysis, i.e., cleft formation within the epidermis or mucous membranes (1). The disease is caused by autoantibodies predominantly directed against keratinocyte surface antigens. Autoantibodies against the cadherin-type adhesion molecules desmoglein 1 (DSG1) and DSG3 are well established to be both necessary and sufficient to induce cell dissociation both in vivo and in vitro (2). Recently, desmocollin 3 (DSC3) was suggested as another relevant cadherin-type antigen in pemphigus (3). Of note, other autoantibodies against nonadhesive molecules such as acetylcholine receptors are present in PV but their pathophysiological significance is not fully understood (4, 5).

DSGs are part of the core complex of desmosomes (6, 7). These distinct cell adhesion sites are abundant in tissues that are exposed to high degrees of mechanical stress, such as the epidermis or the heart muscle. DSGs, together with DSCs, are transmembrane proteins which mediate adhesion by transinteracting with cadherins of the opposing cell. Both homophilic (e.g., DSG3-DSG3) and heterophilic (e.g., DSC3-DSG1) transinteraction have been shown (8–12). Within the desmosome, DSGs and DSCs are anchored to the intracellular plaque proteins plakoglobin, plakophilins, and desmoplakin, the latter of which mediates connection to the intermediate filament cytoskeleton. Thus, desmosomes are essential for the integrity of the specific tissues.

The main pemphigus variant is PV. Patients with autoantibodies against DSG3 typically suffer from mucous membrane erosions, whereas patients with additional DSG1 autoantibodies suffer from both mucous membrane and skin lesions (13). Regarding the pathogenic mechanisms underlying the typical suprabasal acantholysis in PV, 2 main dogmata exist. One attributes loss of cell adhesion solely to direct inhibition of DSG transinteraction by binding of PV Abs (14, 15). This is supported by atomic force microscopy (AFM) experiments demonstrating that under cell-free conditions, IgG fractions of PV patients interfere with DSG3 transinteraction (8, 9). Recently, it was reported that pathogenicity of DSG3 Abs relies on the existence of a consensus domain, which includes a tryptophan residue that may interact with the hydrophobic binding pocket necessary for transinteraction of DSG molecules (16).

Another hypothesis explains cell dissociation merely as a result of cell-signaling events altered by PV-IgG. Indeed, a broad array of signaling events including protein kinase C activation, plakoglobin shuttling, epidermal growth factor signaling, Rho-GTPase inhibition, and cAMP elevation has been described (17–23). A central step required for pemphigus pathogenesis appears to be p38 MAPK activation, which was shown to occur in vitro and in vivo as well as in patient skin lesions (18, 20, 24–26).

Despite the variety of possible therapeutic approaches under experimental conditions, the therapy of pemphigus patients still is based on long-term use of high-dose systemic corticosteroids in combination with other immunosuppressants including azathioprine, mycophenole, cyclophosphamide, and more recently, rituximab (27, 28). Due to the frequently observed adverse reactions, novel and specific treatment options are highly needed.

Recently, we have characterized a DSG-specific peptide termed single peptide (SP) that interferes with transinteraction of DSG molecules in a cell-free system (29). Importantly, 2 linked SP

Conflict of interest: The authors have declared that no conflict of interest exists.
Citation for this article: *J Clin Invest.* doi:10.1172/JCI60139.

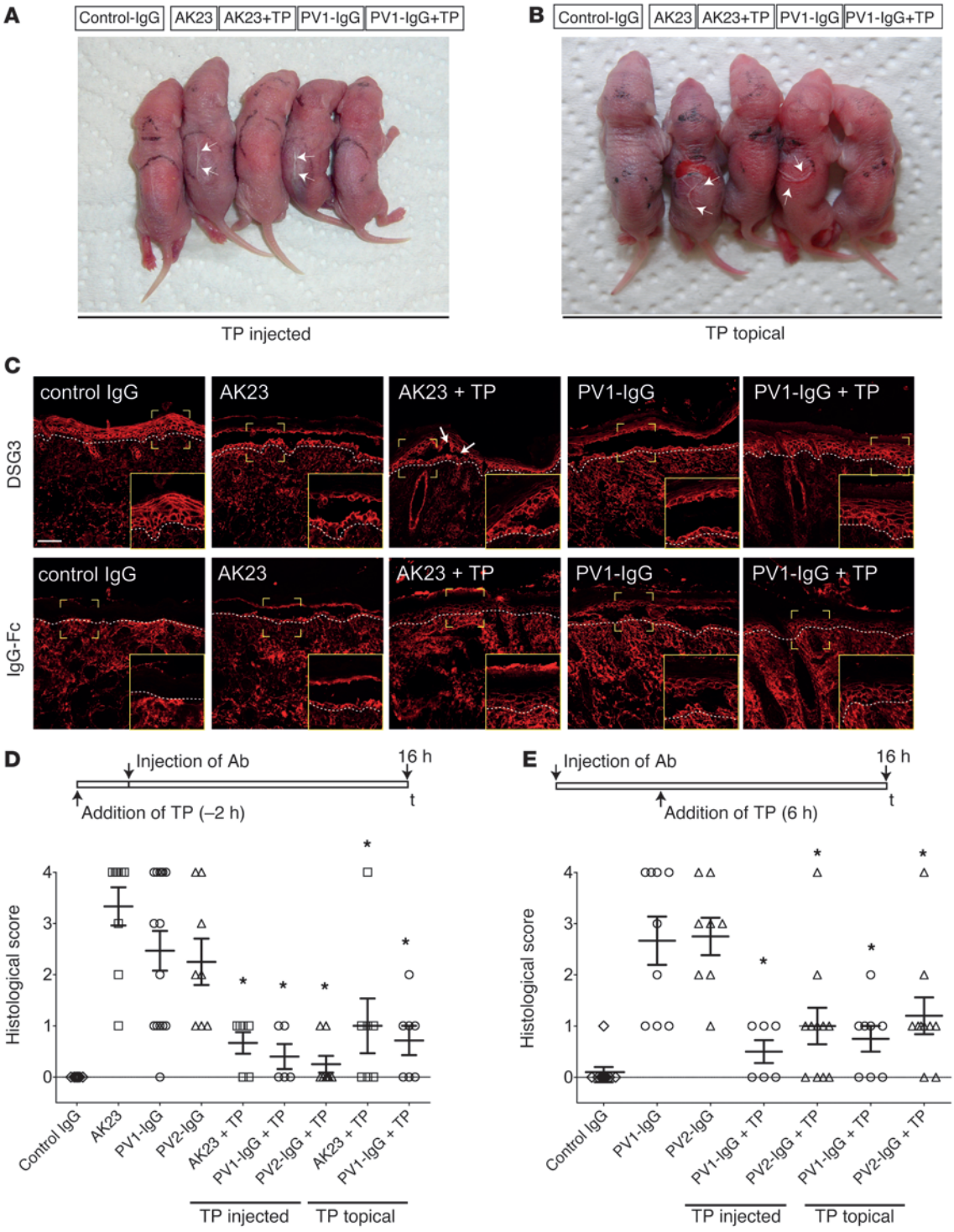

Figure 1

TP blocked acantholysis in vivo. TP blocked macroscopic blistering (arrows) when injected into the back skin of neonatal mice (**A**) or applied topically (**B**). Processing of cryosections revealed typical suprabasal blistering under conditions of AK23 and PV1-IgG injections, but absence or minor blistering (arrows) under conditions of topical TP treatment (**C**, upper panels). Lower panels demonstrate proper IgG deposition within the epidermis following injection of AK23 or PV-IgG and absence of staining in control-IgG–injected animals. Dashed lines represent dermal-epidermal junction. Scale bar: 50 μm (inserts, ×2 magnification). Evaluation of blister size in serial sections under conditions of TP application 2 hours prior to Ab injection (**D**) and 6 hours after Ab injection (**E**). Serial sections of skin samples were evaluated for cleft length and sorted into a score ranging from 0 to 4 as detailed in Methods. Every data point represents 1 injected animal; higher values indicate stronger blistering. **P* < 0.05 Ab injection vs. respective Ab injection + TP.

Table 1
Macroscopic blistering in the murine pemphigus model

	TP pretreatment		TP posttreatment	
	No. mice with gross blisters	No. mice without gross blisters	No. mice with gross blisters	No. mice without gross blisters
Control-IgG	0	11	0	10
AK12	7	2		
AK23 + TP injected	0	6		
AK23 + TP topical	1	6		
PV1-IgG	8	7	5	4
PV1-IgG + TP injected	0	5	0	6
PV1-IgG + TP topical	0	7	1	7
PV2-IgG	3	5	5	3
PV2-IgG + TP injected	0	8	1	10
PV2-IgG + TP topical			1	9

yielding a tandem peptide (TP) abolished loss of transinteraction induced by PV-IgG in vitro. Here, we extended these studies to the in vivo situation in a pemphigus mouse model and investigated the mechanisms underlying the protective effect of TP.

Results

TP abrogated autoantibody-mediated interference of DSG3 transinteraction and blocked acantholysis in vivo. Previously, we designed and extensively characterized a peptide effectively blocking autoantibody-induced loss of DSG3 transinteraction in vitro, which we have termed TP (29). It consists of 2 linked single peptides which, when applied unlinked, interfere with DSG transinteraction (29). To prove the efficacy of TP to block the effect of the Abs used in this study, we applied AFM on recombinant DSG3 molecules and optical trapping of DSG3-coated microbeads on HaCaT keratinocytes (Supplemental Figure 1; supplemental material available online with this article; doi:10.1172/JCI60139DS1). We used AK23, a well-characterized monoclonal DSG3 Ab against the N-terminal adhesive interface of DSG3 derived from an active pemphigus mouse model (30) and an IgG fraction of a PV patient (PV1-IgG) suffering from mucocutaneous disease with autoantibodies against DSG3 and DSG1. Both loss of DSG3 interaction and reduced binding of DSG3-coated microbeads after 30 minutes of AK23 or PV1-IgG incubation were ameliorated by 30 minutes of pretreatment with TP.

Next, we applied TP in vivo. We used the neonatal pemphigus mouse model and injected the back skin of newborn Balb/c mice with AK23 (100 μg/mouse) or PV1-IgG (300 μg/mouse). PV1-IgG induced gross blistering at the injection site upon application of shear stress on the back skin (Nikolsky sign) (Figure 1A). Interestingly, selectively targeting DSG3 by AK23 also was effective to induce Nikolsky-positive blisters in a dose-dependent manner (Figure 1A and Supplemental Figure 2A). However, 50 μl TP preinjection (20 μmol/l) 2 hours before application of Abs abolished gross blistering (Figure 1A and Table 1). To further explore the therapeutic potential of TP, the molecule was also applied topically because cutaneous injection of TP is obviously not a feasible approach for the treatment of pemphigus patients. Although the penetration of peptides through the epidermis is limited and depends on a variety of factors, such as size or polarity, successful delivery, for instance, for insulin, has been demonstrated (31). We therefore applied 2 nmol of TP in linimentum aquosum ointment (a 2-fold dose compared with the injection experiments to account for a potential loss by epidermal penetration) on the back of neonatal mice 2 hours before control-IgG, AK23, and PV1-IgG were injected, respectively. These mice were compared with mice that received the ointment without TP followed by injection of Abs. We confirmed that TP was able to penetrate the upper epidermal layers, as biotin-labeled TP was detectable within the epidermis (Supplemental Figure 2B). Macroscopically, blistering was absent in all but 1 mouse (Figure 1B and Table 1) Also histologically, blistering was drastically reduced (Figure 1C); however, small blisters were slightly more frequent compared with the animals injected with TP. The strictly suprabasal cleavage plane typical for PV was demonstrated by staining DSG3 in cryosections of the back skin (Figure 1C). Human IgG was visualized to guarantee proper Ab deposition (Figure 1C). TP did not pronouncedly affect AK23 or PV1-IgG binding to keratinocytes.

To more thoroughly investigate the effect of TP on suprabasal blister size, a detailed analysis of serial sections of skin samples was performed (Figure 1D) and a second IgG fraction was included (PV2-IgG). Gross blistering by PV2-IgG was prevented by TP similarly to AK23 and PV1-IgG. One section per 100 μm was stained and scored using a scale ranging from 0 to 4 as detailed in Methods until the complete sample was processed. All animals injected with control-IgG yielded a score of zero, as no blistering was evident. Following AK23, PV1-IgG, or PV2-IgG injection, scores of 3.3 ± 0.4, 2.5 ± 0.4, and 2.3 ± 0.5 were determined, respectively. In contrast, TP preinjection reduced scores to 0.7 ± 0.2 (AK23), 0.4 ± 0.2 (PV1-IgG), and 0.3 ± 0.2 (PV2-IgG). Topical treatment was slightly less effective, with values of 1.0 ± 0.5 (AK23) and 0.7 ± 0.3 (PV1-IgG). TP alone did not induce macroscopic or microscopic blisters, even when injected in 10-fold higher doses (200 μmol/l) (Supplemental Figure 2C).

To better mimic the situation in patients, we applied TP 6 hours after addition of autoantibody fractions. Similar to TP preinjection, TP post-treatment significantly reduced gross blistering (Table 1) and microscopic cleavage formation (Figure 1E) independently of whether applied by injection or topically.

TP blocks cell dissociation in cultured keratinocytes. Rearrangement of DSG3 localization in keratinocytes is a typical result of incubation with pemphigus autoantibodies (Figure 2A). Alteration of DSG3 staining in cultured human HaCaT keratinocytes with formation of linear arrays was similarly present 24 hours as well as 48 hours following incubation with AK23. Fragmentation of DSG3 staining was even more prominent after treatment with PV1-IgG and PV2-IgG, but coincubation of TP ameliorated these effects on DSG3 distribution in response to autoantibody treatment. Although overall staining intensity was only mildly increased, DSG3 appeared more regularly distributed along the cell membrane. TP alone had no effect on DSG3 distribution after 48 hours. The monomeric variant of TP, SP, which we have demonstrated to induce loss of cell adhesion (29), did not pronouncedly alter DSG3 distribution after 48 hours. We next measured cell adhesion of HaCaT keratinocytes using dispase-based dissociation assays

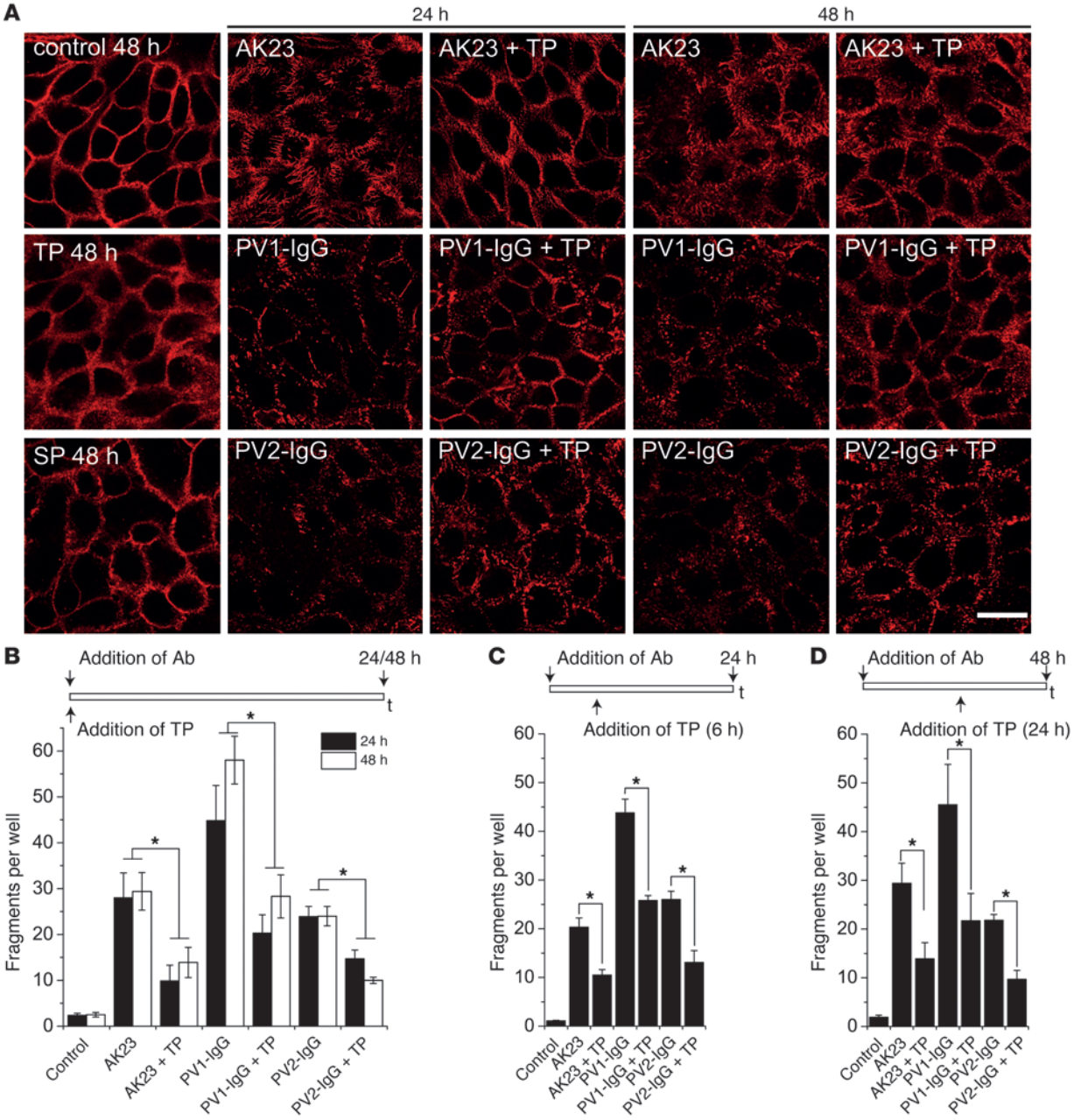

Figure 2

TP ameliorated fragmentation of DSG3 staining and cell dissociation induced by autoantibody application in vitro. (**A**) In cultured HaCaT keratinocytes, fragmentation of DSG3 staining induced by AK23, PV1-IgG, or PV2-IgG was reduced after 24 and 48 hours coincubation with TP. Cells incubated with either TP alone or SP did not demonstrate pronounced changes in the distribution of DSG3. Scale bar: 20 μm. Images are representative of at least 3 experiments. (**B**) Loss of cell adhesion induced by autoantibody treatment for 24 and 48 hours was ameliorated as detected by dispase-based dissociation assays (n = 9–11). Similar results were obtained when TP was applied 6 hours after addition of autoantibodies for 24 hours (**C**) or 24 hours after addition of autoantibodies for 48 hours (**D**). n = 9. *P < 0.05.

(Figure 2B). The monolayers were exposed to defined mechanical stress, and the resulting fragment numbers were quantified. In controls, fragment numbers were 3.2 ± 1.1. AK23, PV1-IgG, or PV2-IgG treatment for 24 hours increased fragment numbers to 28.0 ± 5.4, 55.7 ± 10.6, and 23.9 ± 2.2, respectively. Loss of cell adhesion was significantly reduced by simultaneous application of TP with fragment values of 9.9 ± 3.4 (AK23), 27.0 ± 5.3 (PV1-IgG), and 14.7 ± 1.9 (PV2-IgG). Autoantibody treatment for 48 hours yielded similar results. In a second set of experiments, we added TP 6 hours after starting the incubation with autoantibodies (Figure 2C). Under these conditions, TP also was effective in reducing fragment numbers from 20.3 ± 1.9 to 10.5 ± 1.1 (AK23), from 43.8 ± 2.8 to 25.8 ± 1.0 (PV1-IgG), and from 26.0 ± 1.7 to 13.1 ± 2.4 (PV2-IgG). Similar results were obtained when TP was

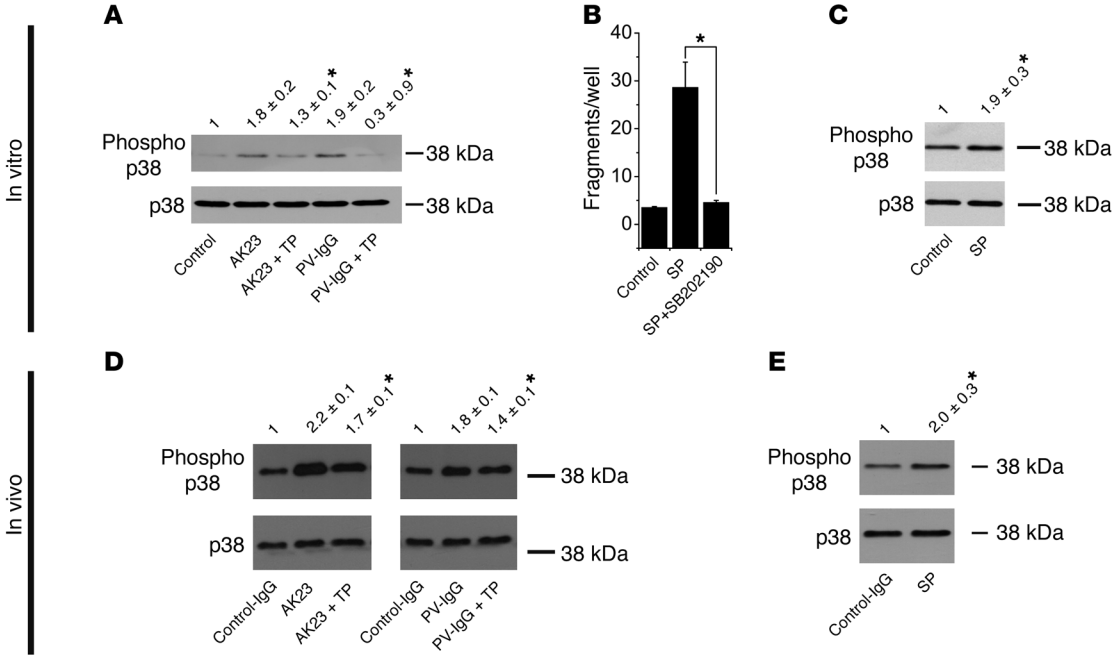

Figure 3

TP inhibited p38 MAPK activation both in vitro and in vivo. (**A**) After 30 minutes of HaCaT incubation with AK23 or PV1-IgG, increased phosphorylation of p38 MAPK was evident. This effect was prevented by 30 minutes of preincubation with TP. Relative band intensity as determined by densitometry is indicated above each lane ($n = 7$; $^*P < 0.05$ vs. autoantibody alone). (**B**) Incubation of HaCaT cells with SP for 24 hours increased fragment numbers, which was inhibited by p38 MAPK inhibitor SB202190 ($n = 6$; $^*P < 0.05$). (**C**) SP increased p38 MAPK phosphorylation after 30 minutes ($n = 5$; $^*P < 0.05$ vs. control). (**D**) Injection of AK23 and PV1-IgG in mice resulted in increased p38 MAPK phosphorylation in skin samples. This effect was ameliorated under conditions of 2 hours of TP preinjection ($n = 5$; $^*P < 0.05$ vs. autoantibody alone). (**E**) Injection of SP increased p38 MAPK phosphorylation ($n = 4$; $^*P < 0.05$ vs. control).

added after 24 hours of a total of 48 hours incubation time with autoantibodies (Figure 2D). TP incubation alone in a 10-fold higher dose (200 μM) only slightly increased fragment numbers compared with autoantibody application (Supplemental Figure 3A). Taken together, these data demonstrate that TP efficiently prevented loss of cell adhesion in vitro and in vivo.

TP prevented p38 MAPK activation in response to autoantibodies in vitro and in vivo. It is still unclear whether direct inhibition of DSG transinteraction or changes in intracellular signaling patterns are the main cause for loss of intercellular adhesion (5, 13). Among the alterations of intracellular signaling molecules, phosphorylation of p38 MAPK at threonine residue 180 and tyrosine 182 is well established (24–26). Therefore, we investigated whether p38 MAPK phosphorylation plays a role in the protective effect of TP in HaCaT cells (Figure 3A). Both AK23 and PV1-IgG induced phosphorylation of p38 MAPK after 30 minutes. Band intensity was increased 1.8 ± 0.2–fold and 1.9 ± 0.2–fold compared with control cells. Interestingly, p38 MAPK activation was blocked by 30 minutes of preincubation of TP (1.3 ± 0.1–fold and 0.9 ± 0.3–fold of controls, respectively).

To further substantiate that specific disruption of DSG transinteraction triggered p38 MAPK activation, we used SP. In dissociation experiments with HaCaT monolayers, SP disrupted monolayer integrity (28.68 ± 5.3 versus 3.5 ± 0.3 fragments in controls) after 24 hours, which was blocked (4.5 ± 0.5 fragments) by simultaneous incubation with the p38 MAPK inhibitor SB202190 (Figure 3B). Similar to AK23 and PV1-IgG, SP also increased p38 MAPK activation after 30 minutes (1.9 ± 0.4–fold of controls; Figure 3C).

Next, we analyzed samples of mice back skin 16 hours following injection of control-IgG, AK23, or PV1-IgG for p38 MAPK activation in Western blots. Compared with control-IgG, the amount of phosphorylated p38 MAPK (phospho–p38 MAPK) increased 2.17 ± 0.03–fold (AK23) and 1.77 ± 0.07–fold (PV1-IgG), respectively (Figure 3D). A 2-hour preinjection of TP significantly reduced the amount of phospho–p38 MAPK to 1.73 ± 0.09–fold of controls and 1.39 ± 0.12–fold of controls, respectively. We next injected SP into mice back skin. We did not detect intraepidermal blistering; however, fragmentation of DSG3 immunostaining was evident (not shown). In addition, SP injection increased p38 MAPK phosphorylation 2.0 ± 0.3–fold of that in controls (Figure 3E).

Since SP increased p38 MAPK phosphorylation and TP decreased phosphorylation induced by autoantibodies, it is reasonable to assume that loss of DSG binding triggers p38 MAPK signaling. An important mechanism for cadherin-mediated binding in general is the insertion of a conserved tryptophan residue at position 2 into a hydrophobic pocket of an opposing cadherin molecule often referred to as tryptophan swap (32–34). Therefore, we hypothesized that addition of tryptophan to the culture medium would have an effect on cell adhesion and p38 MAPK activation. Indeed, p38 MAPK phosphorylation was detectable when 1 μmol/l tryptophan was added for 30 minutes (Figure 4A). This was tryptophan specific, as another aromatic and hydrophobic amino acid, phenylalanine (1 μmol/l), had no effect. Next, we tested whether tryptophan interfered with DSG3 binding in AFM experiments (Figure 4B). Indeed, at concentrations of 1 μmol/l and 20 μmol/l, binding frequency was reduced to 0.75 ± 0.12

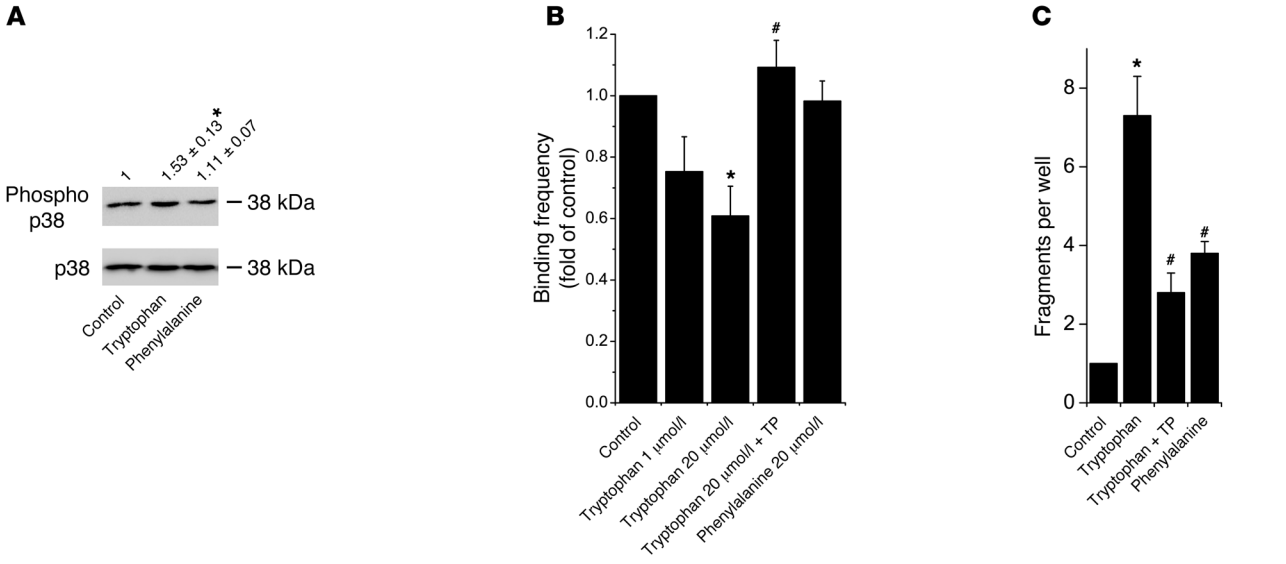

Figure 4

Tryptophan induced p38 MAPK activation and cell dissociation. (**A**) Tryptophan but not phenylalanine increased p38 MAPK phosphorylation in HaCaT cells after 30 minutes (n = 5; $^*P$ < 0.05 vs. control). (**B**) Binding frequency of DSG3 molecules was reduced following 30 minutes tryptophan application as determined by AFM force spectroscopy, which was prevented by TP preincubation for 30 minutes (n = 4–6 tip sample combinations; $^*P$ < 0.05 vs. control; $^{\#}P$ < 0.05 vs. tryptophan, 20 μmol/l). (**C**) Tryptophan increased loss of cell adhesion detected by dispase-based dissociation assays after 24 hours, which was reduced by TP (n = 9; $^*P$ < 0.05 vs. control; $^{\#}P$ < 0.05 vs. tryptophan).

and 0.61 ± 0.10 of controls after 30 minutes, respectively. Furthermore, 30 minutes of TP pretreatment blocked tryptophan-induced loss of DSG binding (1.10 ± 0.09 of controls). Phenylalanine (20 μmol/l) had no effect (0.98 ± 0.09 of controls). Similarly, as measured by dissociation assays, tryptophan increased loss of HaCaT adhesion in a dose-dependent fashion, whereas phenylalanine had minor effects (Figure 4C and Supplemental Figure 3, B and C). Importantly, tryptophan-induced cell dissociation was significantly reduced by TP treatment (7.3 ± 1.0 compared with 2.8 ± 0.5 fragments). These data underscore the results from experiments using SP, indicating that p38 MAPK activation occurs in response to loss of DSG interaction.

Autoantibody treatment induced activation of DSG3-associated p38 MAPK. Since disruption of DSG3 binding led to activation of p38 MAPK, we next investigated whether DSG3 and p38 MAPK interact, which would indicate the existence of a signaling complex involving DSG3. Using proximity ligation assays (PLAs) for detecting close proximity of DSG3 and phospho–p38 MAPK, only few signals (i.e., molecules closer < 40 nm) were visible under control conditions (Figure 5A). However, after incubation with AK23 for 30 minutes, mean numbers of signals increased from 0.09 ± 0.04 per cell in controls to 1.00 ± 0.21 (Figure 5B). Importantly, TP blocked this increase in signals (0.27 ± 0.06). Controls without anti–phospho–p38 MAPK–detecting Ab were negative, whereas in controls without anti-DSG3 detecting, Ab signals were slightly higher, most likely due to the secondary Ab binding to DSG3-attached AK23.

We confirmed these data by immunoprecipitating DSG3 (Figure 5C). No protein was precipitated in pulldowns without capturing Ab. Plakoglobin and p38 MAPK were found in a complex with DSG3 both under control conditions and after AK23 treatment for 30 minutes. In addition, phospho–p38 MAPK was associated with DSG3 in controls but was increased after 30 minutes of AK23 treatment, whereas levels of total DSG3-associated p38 MAPK did not change. Taken together, these data indicate for what we believe is the first time that p38 MAPK is associated with DSG3 and plakoglobin and is phosphorylated in this localization following AK23 binding.

TP inhibits autoantibody- and anisomycin-induced keratin filament retraction. One of the hallmarks in pemphigus is the collapse of the intermediate filament cytoskeleton, which appears detached from desmosomes and clustered around the nucleus (35). Therefore, we investigated the effect of TP on keratin filament retraction (Figure 6A). Compared with controls, after both 24 and 48 hours of PV1-IgG incubation, intermediate filaments were detached from cell borders (visualized by E-cadherin staining). This effect was strongly reduced by simultaneous TP treatment. To quantitate these observations, the distance between the mass of intermediate filament bundles of opposing cells was measured, as indicated in Figure 6B. AK23, as well as both PV1-IgG and PV2-IgG, significantly increased the distance after 24 and 48 hours, and this was abrogated by TP (Figure 6C). In contrast, SP incubation significantly induced cytokeratin retraction after 24 hours, although less pronounced than after autoantibody incubation (Figure 6D).

It is known that keratin filament dynamics are regulated by p38 MAPK (36–38). To explore whether keratin filament retraction in this context is mediated by p38 MAPK, we used anisomycin to activate p38 MAPK in HaCaT cells. Indeed, treatment with 60 μmol/l anisomycin for 6 hours caused robust p38 MAPK activation (Figure 7A), pronounced keratin filament retraction (Figure 7, B and C), and cell dissociation (Figure 7D). These events were indeed mediated by p38 MAPK because they were abrogated by specific inhibition via SB202190 (30 μmol/l). As expected, TP treatment did not affect anisomycin-induced p38 MAPK phosphorylation (Figure 7A). However, TP effectively inhibited keratin filament retraction as well as cell dissociation. Thus, TP blocked keratin filament retraction and cell dissociation in response to both auto-

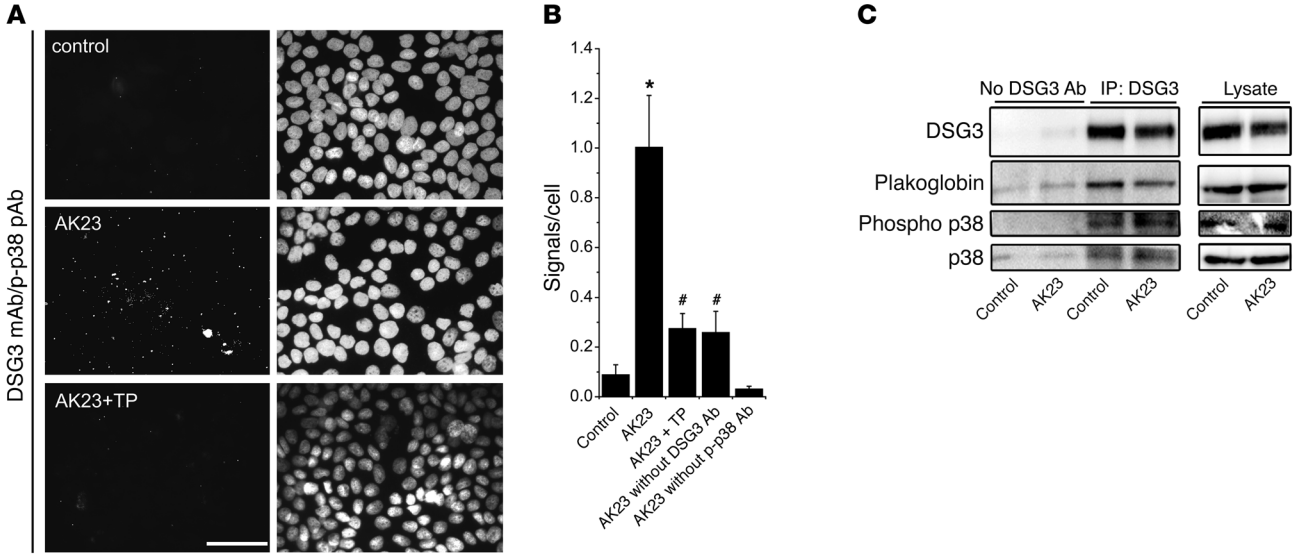

Figure 5

Autoantibody treatment induced activation of DSG3-associated p38 MAPK. (**A**) In PLAs, spatial proximity of DSG3 and phospho–p38 MAPK was evident after AK23 incubation for 30 minutes, which was absent when TP was preincubated for 30 minutes. Scale bar: 50 μm. (**B**) Quantification of signals per total number of cells of 3 independent experiments (5 random fields of view each). **P* < 0.05 vs. control; #*P* < 0.05 vs. AK23. (**C**) IP of DSG3 revealed association of DSG3, plakoglobin, p38 MAPK, and phospho–p38 MAPK. Following 30 minutes of AK23 incubation, DSG3-attached p38 MAPK activity was increased. *n* = 3.

antibody- and anisomycin-mediated p38 MAPK activation. This result suggests that p38 MAPK regulates desmosomal adhesion partially via keratin filament anchorage and that desmosomal cadherin–mediated binding prevents collapse of the intermediate filament cytoskeleton also in part via control of p38 MAPK activity. To further investigate this hypothesis, we characterized the effects of TP on DSG3 arrangement on the keratinocyte cell surface.

TP promoted oligomerization of DSG3 molecules within desmosomes. We next investigated whether TP would inhibit autoantibody-mediated depletion of DSG3, which occurs in HaCaTs when grown for 3 days in high Ca^{2+} medium (39). However, no increased DSG3 levels were notable when TP was coincubated for either 24 or 48 hours with PV1-IgG or PV2-IgG compared with autoantibody treatment alone (Supplemental Figure 4).

Since DSG binding is generally rather weak, we next crosslinked HaCaT cell-surface proteins in vivo with the membrane-impermeable crosslinker ethylene glycol bis(sulfosuccinimidylsuccinate) (sulfo-EGS) (10) and subjected lysates to Western blotting to study oligomerization of DSG3 (Figure 8). Besides the band corresponding to monomeric DSG3 at a size of 130 kDa, we detected 1 band migrating at around 350 to 400 kDa. This band probably represents crosslinked cell-surface DSG3 molecules, since it was absent without application of sulfo-EGS (data not shown). Both bands were reduced to 0.48 ± 0.11 of controls (monomer) and 0.64 ± 0.13 (oligomer) when AK23 was applied for 24 hours (Figure 8A). Interestingly, coincubation of TP led to an increase of oligomeric DSG3 (1.16 ± 0.23 of controls), but not of monomeric DSG3 (0.48 ± 0.08 of controls). Similarly, tryptophan (1 μmol/l) reduced oligomers, which was inhibited by TP (Figure 8B).

To further investigate whether TP promoted oligomerization of DSG3 within desmosomes or within the nondesmosomal pool, we performed Triton X-100 extraction of HaCaT lysates. Both pools were depleted of oligomeric DSG3 by AK23; however, TP increased DSG3 oligomers mainly in the desmosomal pool (Figure 8C). Taken together, the data suggest that TP promoted oligomerization of DSG3 within desmosomes.

Discussion

In this study, we applied a TP consisting of 2 cyclized nonapeptides targeting the adhesive interface of DSGs in vivo. TP, which blocked loss of transinteraction following exposition to pemphigus autoantibodies, efficiently prevented skin blistering by AK23 and PV-IgG when injected intradermally into the back skin of neonatal mice. Most importantly, and for the first time, to our knowledge, this specific approach was also effective when applied topically, rendering it potentially applicable as a treatment option in pemphigus. In addition, TP served to further elucidate the mechanisms by which autoantibodies cause loss of cell cohesion. We targeted DSG3 transinteraction by different approaches and found that direct inhibition of DSG3 binding caused activation of p38 MAPK in vivo and in vitro as well as retraction of keratin filaments, both hallmarks of pemphigus pathogenesis that were blocked by TP. Furthermore, we showed that p38 MAPK associated with DSG3 and in this localization was activated in response to AK23. This indicates the existence of a DSG3-based signaling complex that controls intermediate filament cytoskeleton dynamics dependent on intercellular cohesion.

TP may serve as promising treatment option in pemphigus. Pemphigus is a severe autoimmune disease that potentially leads to death due to uncontrollable epidermal barrier defects and infections. Thus, a constant immunosuppression, commonly reached by steroid application, is pivotal and often necessary for long periods of time. Newer approaches, such as B cell depletion or intravenous application of high doses of IgG, are effective but not primarily applied yet. Thus, to prevent the severe side effects of unspecific immunosuppression, other steroid-sparing approaches are highly appreciated.

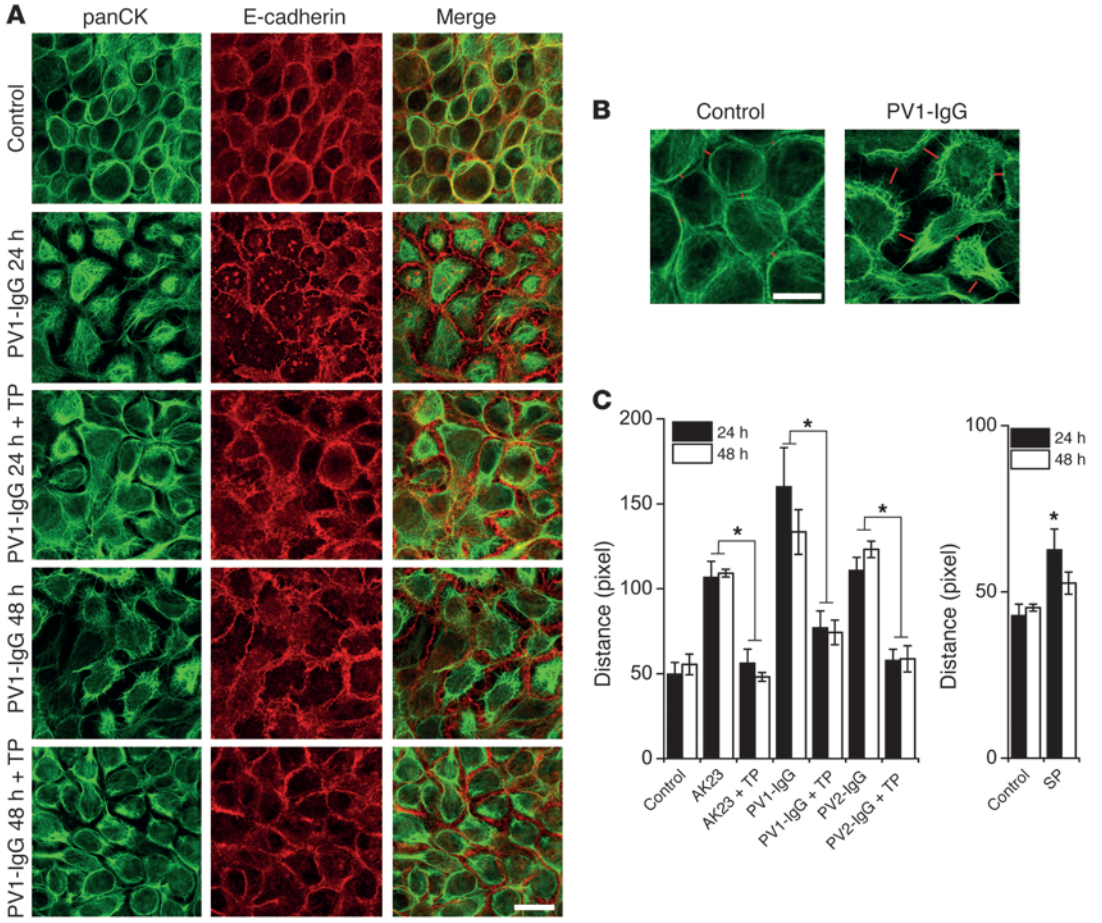

Figure 6
Autoantibody-induced cytokeratin retraction was prevented by TP. (**A**) Keratin retraction evident after 24 hours of PV1-IgG treatment in HaCaT cells was reduced by simultaneous TP application. E-cadherin staining, which was only mildly affected, served to delineate cell membranes. Scale bar: 20 μm. (**B**) Keratin retraction was quantified by measuring the distance between the mass of the keratin bundles (lengths of red lines) in areas of similar cell density as depicted. Scale bar: 10 μm. (**C**) Analysis based on **B** revealed keratin retraction after 24 and 48 hours of AK23, PV1-IgG, and PV2-IgG, which was blocked by TP. Values of 5 random fields of view from 6 independent experiments were obtained (*$P < 0.05$). (**D**) SP increased cytokeratin retraction. Values of 5 random fields of view from 4–5 independent experiments were obtained (*$P < 0.05$ vs. respective control).

TP application abrogated both autoantibody-induced loss of DSG transinteraction and p38 MAPK activation. Thus, 2 main mechanisms underlying pemphigus pathogenesis, i.e., direct inhibition of DSG binding as well as altered intracellular signaling, were prevented by TP. This makes application of TP or similar substances a very attractive and specific therapeutic approach in PV therapy. A topical approach might indeed be feasible because some PV lesions tend to relapse at preferred sites, e.g., the scalp. Especially at these sites, application of TP may be beneficial. Moreover, since TP was also protective in vivo when applied after injection of autoantibodies, it is conceivable that application in developing lesions is effective too. Further studies need to determine and to optimize the delivery efficiency and potential toxicity in human skin.

DSG3 regulates p38 MAPK activity to control keratin filament dynamics. A relatively new concept proposes that desmosomal proteins, especially the desmosomal cadherins, modulate intracellular signaling events (40). It has been shown that DSG1 suppresses EGFR signaling in the more superficial epidermal layers (41). Furthermore, DSC2 has recently been demonstrated to prevent PI3K/Akt-mediated phosphorylation of β catenin (42). Data from this study support this concept because TP, by promoting DSG transinteraction, blunted p38 MAPK activation in response to the DSG3-specific autoantibody AK23, indicating that DSG3 is involved in regulation of p38 MAPK activity. In line with this observation, SP, which prevents DSG transinteraction, increased p38 MAPK activation. Thus, most likely, loss of DSG transinteraction is the trigger for p38 MAPK activation, which is further underscored by our data showing that tryptophan, to block the tryptophan swap important for cadherin transinteraction (43), had the same effect. This places p38 MAPK activation downstream of direct inhibition of DSG3 binding in pemphigus. In this context, it is very interesting that p38 MAPK associates with DSG3 and plakoglobin and thus may form a DSG3-based signaling complex that is present under resting conditions. Upon autoantibody binding, DSG3-associated p38 MAPK is phosphorylated and thereby activated. The fact that, similarly to TP in this study, inhibition of p38 MAPK was found to prevent PV-IgG–induced loss of cell adhesion and skin blister-

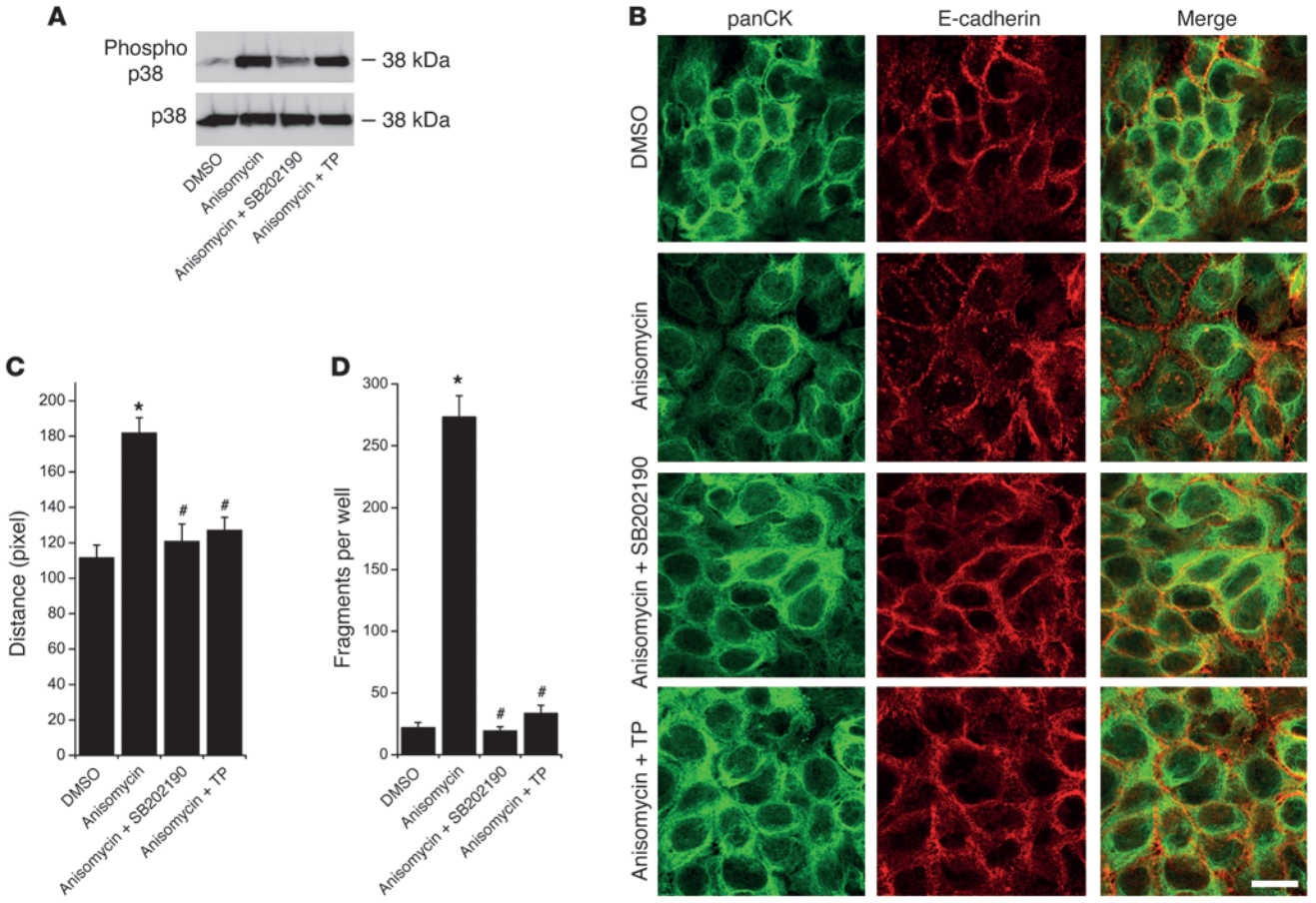

Figure 7

TP inhibited keratin retraction and loss of cell adhesion induced by anisomycin-mediated p38 MAPK activation. (**A**) Anisomycin-induced p38 MAPK activation after 6 hours was blocked by the specific p38 MAPK inhibitor SB202190, but not by simultaneous TP treatment $n = 3$. (**B**) Keratin retraction by anisomycin was inhibited by both SB202190 and TP. Scale bar: 20 μm. (**C**) Statistical analysis of keratin retraction from 6 independent experiments with 5 fields of view each. $^{*}P < 0.05$ vs. DMSO; $^{\#}P < 0.05$ vs. anisomycin. (**D**) Loss of cell adhesion by anisomycin was prevented by both SB202190 and TP as detected by dispase-based dissociation assays. $n = 9$. $^{*}P < 0.05$ vs. DMSO; $^{\#}P < 0.05$ vs. anisomycin.

ing both in vitro and in vivo (24, 25) suggests that a signaling loop exists in which p38 MAPK is activated by loss of DSG transinteraction, which in turn destabilizes desmosomal adhesion.

In this context, the cytoskeleton may play an important role. The intermediate filament network tethering desmosomes to the cell membrane has been demonstrated to disintegrate in response to p38 MAPK activation (36). Since a tight anchorage of intermediate filaments to the desmosomal complex is necessary for maintaining strong adhesion (44) and retraction of the intermediate filament network is a hallmark of pemphigus (35), p38 MAPK–mediated collapse of these cytoskeletal structures may be a central event for loss of cell adhesion. This idea is supported by the data showing that anisomycin-mediated p38 MAPK activation induced both keratin filament retraction and loss of cell adhesion.

However, it is noteworthy that TP, without affecting p38 MAPK activation in response to anisomycin, still was effective in abrogating keratin filament retraction and loss of cell adhesion. This observation indicates that desmosomal adhesion and intermediate filament cytoskeleton integrity are linked to each other in reciprocal fashion. Augmented oligomerization of desmosomal DSG3, which we detected in response to TP, may therefore increase intercellular adhesion not only directly but also by controlling keratin filament anchorage. Since TP reduced both autoantibody-induced p38 MAPK activation and autoantibody- and anisomycin-mediated keratin filament retraction, the data also raise the possibility that other signaling pathways involved in keratin filament retraction are modulated by DSG3 binding. It has been shown that a desmoplakin point mutation (Ser2849Gly) exhibited strongly increased binding to intermediate filaments and in addition rendered desmosomes super-adhesive (45), a state that also protects against loss of cell adhesion in pemphigus (39, 46). Since the desmoplakin point mutation is located within a PKC consensus sequence, one may speculate that PKC-mediated phosphorylation of desmoplakin may be involved in keratin filament retraction and this process may be modulated by TP via stabilization of DSG3 binding.

Nevertheless, p38 MAPK may regulate desmosomal adhesion independently of intermediate filaments. For example, p38 MAPK phosphorylation has been shown to alter organization of the actin cytoskeleton via heat shock protein 27 (24) and actin filament dynamics, especially within the peripheral junction-associated actin belt were shown to affect autoantibody-induced loss of cell adhesion (47).

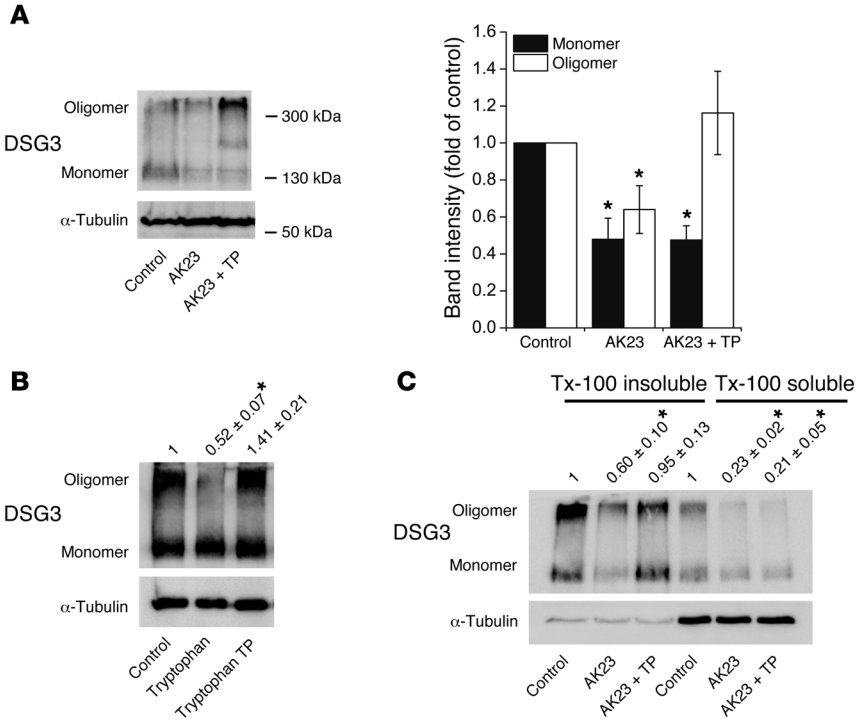

Figure 8
TP promoted oligomerization of desmosomal DSG3 on the cell surface. (**A**) Following cross-linking of membrane proteins, both monomeric and oligomeric DSG3 molecules were detectable by Western blotting (left panel shows representative blot). After 24 hours of AK23, both forms were reduced; however, TP coincubation increased the amount of DSG3 oligomers. Right panel shows band densities of 5 independent experiments. *$P < 0.05$ vs. respective control. (**B**) Tryptophan reduced DSG3 oligomers after 24 hours, which was inhibited by TP coincubation. Numbers demonstrate relative oligomeric DSG3 band intensity of 4 independent experiments. *$P < 0.05$ vs. controls. (**C**) Proteins were divided into desmosomal and nondesmosomal pools by Triton X-100 extraction. TP increased oligomers only in the Triton X-100–insoluble (e.g., desmosomal) pool. Numbers demonstrate fold of controls of oligomeric DSG3 band intensity of 5 independent experiments. *$P < 0.05$ vs. controls.

Moreover, p38 MAPK has been demonstrated to be involved in autoantibody-induced DSG3 internalization in pemphigus (48).

Taken together, data from this study demonstrate that a topically administered approach to specifically targeting DSG-mediated binding not only is effective in limiting pemphigus autoantibody–induced skin blistering in vivo, but also serves as a good tool for studying the mechanisms underlying pemphigus pathogenesis.

Methods

Test reagents. The monoclonal DSG3 Ab AK23 (30) was purchased from Biozol and used at 75 μg/ml in vitro. PV sera were drawn from patients with active PV suffering from both oral and skin lesions. Both sera were tested by ELISA for DSG1 and DSG3 Abs (Table 2) and applied at 0.5 mg/ml in vitro. PV-IgG was purified as reported before (49). Anisomycin (Sigma-Aldrich) was applied at 60 μmol/l.

TP was characterized before (29) and synthesized by Bachem GmbH. It consisted of 2 so-called SP, with the sequence LNSMGQD corresponding to amino acids 81–86 of DSG1 mimicking a transinteracting DSG. Because of high sequence homology at this position for DSG1 and DSG3, SP is supposed to bind both isoforms (29). A cysteine residue was added to the C- and N-terminal ends, which were connected by disulfide bonds yielding a cyclized peptide. In the combined TP, 2 SP are interconnected by a flexible amino hexan linker interposed between 2 cysteine residues. TP was applied at 20 μmol/l, a concentration experimentally determined to block PV-IgG–mediated direct inhibition of DSG3 transinteraction (29). SP was applied at 200 μmol/l for topical treatment; 2 nmol TP in 100 mg linimentum aquosum ointment per mouse was freshly prepared prior to usage. For some experiments, TP was labeled with sulfo-NHS-biotin (Thermo Fisher Scientific) according to the manufacturer's instructions, dialyzed extensively afterwards to remove excess biotin, and applied topically. Tryptophan and phenylalanine were purchased from Sigma-Aldrich and applied at concentrations from 1 to 200 μmol/l.

Neonatal mouse model. Newborn Balb/C mice weighing 1.4–1.8 g were injected intradermally into the back skin with 50 μl PV1-IgG or PV2-IgG (6 mg/ml each), AK23 (2 mg/ml, 0.4 mg/ml, or 0.08 mg/ml), or control-IgG of a healthy donor (6 mg/ml) in PBS. SP was injected at 200 μmol/l (50 μl PBS). TP was preinjected at 20 μmol/l (in 50 μl PBS) 2 hours before injection of IgG fractions. Controls and IgG-only conditions received 50 μl of PBS 2 hours before. For some experiments, 2 nmol TP was mixed in 100 mg of linimentum aquosum and applied as ointment on the back skin 2 hours before injection of IgG fractions. As controls, linimentum aquosum was mixed with PBS and also applied 2 hours before. In another set of experiments, TP was either injected or applied topically 6 hours after injection of PV1-IgG or PV2-IgG. Sixteen hours after injection of autoantibodies, the injection site was exposed to defined mechanical stress to induce intraepidermal separation (Nikolsky sign). Mice were sacrificed, and back skin was harvested. Skin explants were embedded in cryo mounting medium (Reichert-Jung) and frozen in liquid nitrogen. Parts of the samples were homogenized in Laemmli buffer with 10 strokes of a homogenizer and subjected to Western blotting experiments.

Processing of cryosamples and scoring of blister size. Samples were cut with a cryostat (Reichert-Jung). Every 100 μm, 2 sections were stained with 1% toluidine blue solution and evaluated for intraepidermal separation until the complete sample was processed. Each section was then evaluated and sorted in a scoring system according to the following guidelines: absence of intraepidermal separation, score 0; cleft size covering 1%–25% of total section length, score 1; cleft size between 26% and 50% of section length, score 2; cleft size between 51% and 75%, score 3; and cleft size over 75%, score 4. If different numbers were obtained within 1 sample, the highest number was counted.

Table 2
ELISA scores of PV-IgG fractions

	DSG1 [U/ml]	DSG3 [U/ml]
PV1-IgG	711	5,542
PV2-IgG	375	11,550

Additional sections were subjected to immunodetection of DSG3 and IgG-Fc as described before (20). AK23 (1:100) was used together with a Cy3-linked goat anti-mouse secondary Ab (1:600; Dianova) to detect murine DSG3. Deposition of IgG was evaluated using Cy3-linked goat anti-human (PV-IgG, control-IgG) or Cy3-linked goat anti-mouse Abs (AK23) in 1:600 dilution (both Dianova). TP-biotin was detected by Alexa Fluor 488–conjugated streptavidin (Life Technologies). Fluorescence images were acquired using a SP5 confocal setup equipped with a HCX PL APO CS ×40 1.25 oil objective (both Leica).

AFM and optical trapping. The principles of cell-free binding studies of recombinant DSGs have been outlined earlier (8). In brief, recombinant DSG3-Fc molecules were attached to a mica substrate and to the sharp tip of soft (spring constants 0.01 and 0.03 N/m) silicon nitride cantilevers (MSCT probes; Bruker) via a flexible polyethylenglycol linker (50). Tip and mica were repeatedly brought in contact and retracted using a Bioscope AFM attached to a Nanoscope III controller (Bruker).

Force distance cycles were performed at 1 Hz, with 100 ms contact time of the cantilever on the mica sheet. Adhesion events between recombinant DSG3 molecules were detected by a downward bent of the AFM cantilever, which abruptly jumps back into the neutral position (indicating an unbinding event) once the cantilever is retracted far enough from the mica surface (Supplemental Figure 1A). The numbers of these unbinding events per total number of approach-retract cycles yielded the binding frequency. In total, experiments were carried out on at least 3 different cantilever/mica combinations, yielding more than 1,500 approach/retract cycles per condition.

To determine DSG3-mediated adhesion on a cellular level, 2.4 μm protein A Dynabeads (Life Technologies) were coated with recombinant DSG3-Fc molecules as reported elsewhere (51). Beads were allowed to settle on the surface of HaCaT keratinocytes to allow for contact formation. Subsequently, beads were exposed to the beam of a 1,064 nm Nd:Yag laser at 42 mW in the focal plane of a home-built laser tweezer setup. This allowed for the movement of unbound beads, whereas the beads tightly attached to the cells were not displaceable. The percentage of bound beads is a measure for DSG3-mediated adhesion.

Cell culture and immunofluorescence studies. HaCaT human keratinocytes were seeded in 12-well plates and cultured as described previously (20). Fully confluent cells were subjected to immunofluorescence studies 3 to 5 days after seeding as described elsewhere (51). A monoclonal DSG3 Ab (Life Technologies) was used as primary Ab at 1:100 dilution. Cy3-coupled secondary Abs (1:600) were from Dianova. Keratin filaments were visualized by an FITC-conjugated monoclonal pan-cytokeratin Ab (Sigma-Aldrich). Monolayers were imaged using a LSM510 META equipped with a Plan Apochromat ×63 oil objective (both Zeiss).

PLAs. Spatial proximity of DSG3 and phospho–p38 MAPK was investigated using the Duolink in situ kit (Olink Bioscience) according to the manufacturer's instructions. The technique is based on the ligation and amplification of DNA oligonucleotides attached to secondary Abs that bind to primary Abs of the 2 proteins of interest. DNA ligation and amplification can only occur if the 2 proteins are in close proximity (<40 nm) and can be detected by fluorescent DNA probes. Primary Abs used were mouse monoclonal DSG3 Ab (Life Technologies) and rabbit phospho–p38 MAPK (Cell Signaling). Images were acquired with a Zeiss Axiophot microscope using a ×40 Plan Neofluar objective and a Zeiss Axiocam Hrc CCD camera at strictly the same settings.

Dissociation assays. Dispase-based dissociation assays were performed in order to quantify intercellular adhesive strength in vitro. Briefly, confluent HaCaT monolayers were washed twice in HBSS (Sigma-Aldrich) and incubated with Dispase II (>2.4 U/ml, Sigma-Aldrich) in HBSS for 30 minutes at 37°C to release the monolayer from the well bottom. Dispase solution was carefully replaced by HBSS. The monolayer was then mechanically stressed by pipetting up and down 5 times using a 1-ml pipet. The resulting numbers of fragments are a measure for loss of intercellular adhesion.

In vivo crosslinking of membrane proteins. To crosslink membrane proteins, the membrane impermeable crosslinker ethylene glycol bis(sulfosuccinimidylsuccinate) (sulfo-EGS; Thermo Fisher Scientific) was added to HaCaT keratinocytes. Cells were treated with Abs, TP, or amino acids for indicated times. After washing with PBS containing 1.8 mmol/l Ca^{2+}, 1 mmol/l sulfo-EGS in PBS/Ca^{2+} was added for 10 minutes. The reaction was stopped by adding 1 mol/l Tris solution (pH 7.5). Cells were scraped in Laemmli buffer, sonicated, and subjected to Western blotting.

IP. After incubation with PBS or AK23 for 30 minutes, HaCaTs were washed with ice-cold PBS and incubated for 30 minutes with prechilled precipitation buffer (10% NP-40 Alternative [EMD Biosciences], 0.5 M Tris-HCl, 1.5 M NaCl, 10% SDS, 0.5 M EDTA), to which protease and phosphatase inhibitors (cOmplete Tablets; Roche) were freshly added. Cells were scraped, and the lysate was clarified by centrifugation at 18,000 *g* for 5 minutes at 4°C. The supernatant was transferred to fresh reaction vials, and the protein concentration was determined using BCA-Kit (Thermo Fisher Scientific). For IP with the polyclonal DSG3 Ab, cell lysates with 600 μg of total protein amount were precleaned (for 1 hour and 4°C) by incubation with TrueBlot anti-rabbit IgG IP beads (eBioscience). The supernatant was incubated for 3 hours at 4°C with 1 μg of DSG3 Ab. To each sample, 40 μl of beads was added and overnight incubation at 4°C was carried out on a rocker platform. The beads with attached immunoprecipitated complexes were collected by centrifugation at 6,800 *g* for 5 minutes, washed 3 times with cold washing buffer (1% NP-40-Alternative, 0.5 M Tris-HCl, 1.5 M NaCl, 10% SDS, 0.5 M EDTA), resuspended in ×3 Laemmli buffer, and subjected to Western blotting as outlined below.

Western blotting. Cells and tissue material were lysed in Laemmli buffer and subjected to gel electrophoresis and blotting following normalization of protein amounts according to standard procedures. Primary Abs applied were phospho–Thr180/Tyr182-specific rabbit p38 MAPK pAb and non–phospho-specific rabbit p38 MAPK pAb (both Cell Signaling), DSG3 pAb (Santa Cruz Biotechnology Inc.), α-tubulin mAb (Abcam), and GAPDH mAb (Sigma-Aldrich). Either a polyclonal, HRP-coupled goat anti rabbit Ab (Cell Signaling) or a goat anti mouse mAb (Dianova) served as secondary Abs. Membranes were developed using the ECL System (GE Healthcare).

Image processing and statistics. Images were processed using Photoshop CS4 and Illustrator CS5 (both Adobe Systems). Data shown are mean ± SEM. Statistical analysis of 2-group differences was performed using Mann-Whitney rank-sum test and of multiple groups using Kruskal-Wallis test followed by Dunn's post-hoc test. If values were Gaussian-distributed, 1-way ANOVA was performed, followed by Bonferroni's correction. Data were analyzed with Prism (Graph Pad Software). Statistical significance was assumed at $P < 0.05$.

Study approval. All experiments were carried out with permission of the Government of Lower Franconia (Az.:55.2-2531.01-4/10) and of the Government of Upper Bavaria (Az. 55.2-1-54-2532-80-11), Germany.

Acknowledgments

We thank Lisa Bergauer, Tetjana Frantzeskakis, Veronika Heimbach, Claudia Mayerhofer, and Sabine Mühlsimer for excellent technical assistance. Experiments were funded by the Deutsche Forschungsgemeinschaft (SFB 487, TP B5, and SP1300-1).

Received for publication July 22, 2011, and accepted in revised form November 8, 2012.

Address correspondence to: Jens Waschke, Institute of Anatomy and Cell Biology, Pettenkoferstrasse 11, 80336 Munich, Germany. Phone: 49.89.5160.4811; Fax: 49.89.5160.4802; E-mail: jens.waschke@med.uni-muenchen.de.

1. Stanley JR, Amagai M. Pemphigus, bullous impetigo, and the staphylococcal scalded-skin syndrome. *N Engl J Med*. 2006;355(17):1800–1810.
2. Sharma P, Mao X, Payne AS. Beyond steric hindrance: The role of adhesion signaling pathways in the pathogenesis of pemphigus. *J Derm Sci*. 2007; 48(1):1–14.
3. Rafei D, et al. IgG autoantibodies against Desmocollin 3 in pemphigus sera induce loss of keratinocyte adhesion. *Am J Pathol*. 2011;178(2):718–723.
4. Kalantari-Dehaghi M, et al. New targets of pemphigus vulgaris antibodies identified by protein array technology. *Exp Dermatol*. 2011;20(2):154–156.
5. Amagai M, et al. Are desmoglein autoantibodies essential for the immunopathogenesis of pemphigus vulgaris, or just "witnesses of disease"? *Exp Dermatol*. 2006;15(10):815–831.
6. Thomason HA, Scothern A, McHarg S, Garrod DR. Desmosomes: adhesive strength and signalling in health and disease. *Biochem J*. 2010;429(3):419–433.
7. Delva E, Tucker DK, Kowalczyk AP. The desmosome. *Cold Spring Harb Perspect Biol*. 2009; 1(2):a002543.
8. Spindler V, et al. Desmocollin 3-mediated binding is crucial for keratinocyte cohesion and is impaired in pemphigus. *J Biol Chem*. 2009;284(44):30556–30564.
9. Heupel WM, Zillikens D, Drenckhahn D, Waschke J. Pemphigus vulgaris IgG directly inhibit desmoglein 3-mediated transinteraction. *J Immunol*. 2008; 181(3):1825–1834.
10. Nie Z, Merritt A, Rouhi-Parkouhi M, Tabernero L, Garrod D. Membrane-impermeable cross-linking provides evidence for homophilic, isoform-specific binding of desmosomal cadherins in epithelial cells. *J Biol Chem*. 2011;286(3):2143–2154.
11. Syed SE, Trinnaman B, Martin S, Major S, Hutchinson J, Magee AI. Molecular interactions between desmosomal cadherins. *Biochem J*. 2002; 362(Pt 2):317–327.
12. Chitaev NA, Troyanovsky SM. Direct Ca2+-dependent heterophilic interaction between desmosomal cadherins, desmoglein and desmocollin, contributes to cell-cell adhesion. *J Cell Biol*. 1997; 138(1):193–201.
13. Waschke J. The desmosome and pemphigus. *Histochem Cell Biol*. 2008;130(1):21–54.
14. Mahoney MG, Wang Z, Rothenberger K, Koch PJ, Amagai M, Stanley JR. Explanations for the clinical and microscopic localization of lesions in pemphigus foliaceus and vulgaris. *J Clin Invest*. 1999; 103(4):461–468.
15. Wu H, et al. Protection against Pemphigus Foliaceus by desmoglein 3 in neonates. *N Engl J Med*. 2000; 343(1):31–35.
16. Yamagami J, Payne AS, Kacir S, Ishii K, Siegel DL, Stanley JR. Homologous regions of autoantibody heavy chain complementarity-determining region 3 (H-CDR3) in patients with pemphigus cause pathogenicity. *J Clin Invest*. 2010;120(11):4111–4117.
17. Osada K, Seishima M, Kitajima Y. Pemphigus IgG activates and translocates protein kinase C from the cytosol to the particulate/cytoskeleton fractions in human keratinocytes. *J Invest Dermatol*. 1997; 108(4):482–487.
18. Chernyavsky AI, Arredondo J, Kitajima Y, Sato-Nagai M, Grando SA. Desmoglein versus non-desmoglein signaling in pemphigus acantholysis: characterization of novel signaling pathways downstream of pemphigus vulgaris antigens. *J Biol Chem*. 2007;282(18):13804–13812.
19. Spindler V, Waschke J. Role of Rho GTPases in desmosomal adhesion and pemphigus pathogenesis. *Ann Anat*. 2011;193(3):177–180.
20. Spindler V, Vielmuth F, Schmidt E, Rubenstein DS, Waschke J. Protective endogenous cyclic adenosine 5′-monophosphate signaling triggered by pemphigus autoantibodies. *J Immunol*. 2010;185(11):6831–6838.
21. de Bruin A, et al. Plakoglobin-dependent disruption of the desmosomal plaque in pemphigus vulgaris. *Exp Dermatol*. 2007;16(6):468–475.
22. Williamson L, et al. Pemphigus vulgaris identifies plakoglobin as key suppressor of c-Myc in the skin. *EMBO J*. 2006;25(14):3298–3309.
23. Caldelari R, et al. A central role for the armadillo protein plakoglobin in the autoimmune disease pemphigus vulgaris. *J Cell Biol*. 2001;153(4):823–834.
24. Berkowitz P, et al. Desmosome signaling. Inhibition of p38MAPK prevents pemphigus vulgaris IgG-induced cytoskeleton reorganization. *J Biol Chem*. 2005;280(25):23778–23784.
25. Berkowitz P, Hu P, Warren S, Liu Z, Diaz LA, Rubenstein DS. p38MAPK inhibition prevents disease in pemphigus vulgaris mice. *Proc Natl Acad Sci U S A*. 2006;103(34):12855–12860.
26. Berkowitz P, Diaz LA, Hall RP, Rubenstein DS. Induction of p38MAPK and HSP27 phosphorylation in pemphigus patient skin. *J Invest Dermatol*. 2007;128(3):738–740.
27. Kasperkiewicz M, Schmidt E. Current treatment of autoimmune blistering diseases. *Curr Drug Discov Technol*. 2009;6(4):270–280.
28. Schmidt E, Goebeler M, Zillikens D. Rituximab in severe pemphigus. *Ann N Y Acad Sci*. 2009; 1173:683–691.
29. Heupel W-M, Müller T, Efthymiadis A, Schmidt E, Drenckhahn D, Waschke J. Peptides targeting the desmoglein 3 adhesive interface prevent autoantibody-induced acantholysis in pemphigus. *J Biol Chem*. 2009;284(13):8589–8595.
30. Tsunoda K, et al. Induction of pemphigus phenotype by a mouse monoclonal antibody against the amino-terminal adhesive interface of desmoglein 3. *J Immunol*. 2003;170(4):2170–2178.
31. Benson HAE, Namjoshi S. Proteins and peptides: Strategies for delivery to and across the skin. *J Pharm Sci*. 2008;97(9):3591–3610.
32. Boggon TJ, Murray J, Chappuis-Flament S, Wong E, Gumbiner BM, Shapiro L. C-Cadherin ectodomain structure and implications for cell adhesion mechanisms. *Science*. 2002;296(5571):1308–1313.
33. Shapiro L, et al. Structural basis of cell-cell adhesion by cadherins. *Nature*. 1995;374(6520):327–337.
34. Al-Amoudi A, Frangakis AS. Structural studies on desmosomes. *Biochem Soc Trans*. 2008;36(pt 2):181–187.
35. Wilgram GF, Caulfield JB, Lever WF. An electron microscopic study of acantholysis in pemphigus vulgaris. *J Invest Dermatol*. 1961;36:373–382.
36. Woll S, Windoffer R, Leube RE. p38 MAPK-dependent shaping of the keratin cytoskeleton in cultured cells. *J Cell Biol*. 2007;177(5):795–807.
37. Menon MB, et al. p38 MAP kinase and MAPKAP kinases MK2/3 cooperatively phosphorylate epithelial keratins. *J Biol Chem*. 2010; 285(43):33242–33251.
38. Strnad P, Windoffer R, Leube RE. Induction of rapid and reversible cytokeratin filament network remodeling by inhibition of tyrosine phosphatases. *J Cell Sci*. 2002;115(pt 21):4133–4148.
39. Spindler V, Endlich A, Hartlieb E, Vielmuth F, Schmidt E, Waschke J. The extent of desmoglein 3 depletion in pemphigus vulgaris is dependent on Ca(2+)-induced differentiation: a role in suprabasal epidermal skin splitting? *Am J Pathol*. 2011; 179(4):1905–1916.
40. Müller EJ, Williamson L, Kolly C, Suter MM. Outside-in signaling through integrins and cadherins: a central mechanism to control epidermal growth and differentiation? *J Invest Dermatol*. 2008; 128(3):501–516.
41. Getsios S, et al. Desmoglein 1-dependent suppression of EGFR signaling promotes epidermal differentiation and morphogenesis. *J Cell Biol*. 2009; 185(7):1243–1258.
42. Kolegraff K, Nava P, Helms MN, Parkos CA, Nusrat A. Loss of desmocollin-2 confers a tumorigenic phenotype to colonic epithelial cells through activation of Akt/{beta}-catenin signaling. *Mol Biol Cell*. 2011;22(8):1121–1134.
43. Harrison OJ, et al. Two-step adhesive binding by classical cadherins. *Nat Struct Mol Biol*. 2010; 17(3):348–357.
44. Huen AC, et al. Intermediate filament-membrane attachments function synergistically with actin-dependent contacts to regulate intercellular adhesive strength. *J Cell Biol*. 2002;159(6):1005–1017.
45. Hobbs RP, Green KJ. Desmoplakin regulates desmosome hyperadhesion. *J Invest Dermatol*. 2012; 132(2):482–485.
46. Cirillo N, Lanza A, Prime SS. Induction of hyperadhesion attenuates autoimmune-induced keratinocyte cell-cell detachment and processing of adhesion molecules via mechanisms that involve PKC. *Exp Cell Res*. 2010;316(4):580–592.
47. Gliem M, Heupel W-M, Spindler V, Harms GS, Waschke J. Actin reorganization contributes to loss of cell adhesion in pemphigus vulgaris. *Am J Physiol Cell Physiol*. 2010;299(3):C606–C613.
48. Jolly PS, et al. p38MAPK signaling and desmoglein-3 internalization are linked events in pemphigus acantholysis. *J Biol Chem*. 2010;285(12):8936–8941.
49. Waschke J, Bruggeman P, Baumgartner W, Zillikens D, Drenckhahn D. Pemphigus foliaceus IgG causes dissociation of desmoglein 1-containing junctions without blocking desmoglein 1 transinteraction. *J Clin Invest*. 2005;115(11):3157–3165.
50. Wildling L, et al. Linking of sensor molecules with amino groups to amino-functionalized AFM tips. *Bioconjug Chem*. 2011;22(6):1239–1248.
51. Spindler V, Drenckhahn D, Zillikens D, Waschke J. Pemphigus IgG causes skin splitting in the presence of both desmoglein 1 and desmoglein 3. *Am J Pathol*. 2007;171(3):906–916.